

# Nucleon-Nucleon interactions from effective field theory

José A. Oller<sup>#1</sup>

*Departamento de Física. Universidad de Murcia.  
E-30071, Murcia. Spain.*

## Abstract

We have established a new convergent scheme to treat analytically nucleon-nucleon interactions from a chiral effective field theory. The Kaplan-Savage-Wise (KSW) amplitudes are resummed to fulfill the unitarity or right hand cut to all orders below pion production threshold. This is achieved by matching order by order in the KSW power counting the general expression of a partial wave amplitude with resummed unitarity cut with the inverses of the KSW amplitudes. As a result, a new convergent and systematic KSW expansion is derived for an on-shell interacting kernel  $\mathcal{R}$  in terms of which the partial waves amplitudes are computed. The agreement with data for the S-waves is fairly good up to laboratory energies around 350 MeV and clearly improves and reestablishes the phenomenological success of the KSW amplitudes when treated within this scheme.

---

<sup>#1</sup>email: oller@um.es

# 1 Introduction

Effective field theories are the standard method to deal with strong interactions in the non-perturbative regime. As paradigm we have SU(2) Chiral Perturbation Theory (CHPT) for pion physics [1, 2, 3], where a convergent power counting is established in terms of derivatives, insertions of quark mass matrix and external sources. This has also been applied to pion-nucleon interactions with baryon number,  $B$ , equal to 1 [4]. Its extension to nucleon-nucleon physics [5, 6, 7, 8, 9] is not straightforward due to the appearance of two new scales: the large scattering lengths of the S-waves and the large nucleon mass,  $M$ . The latter can be easily handled for  $B=1$  although this is no longer the case for  $B>1$  [5]. Large efforts have been devoted during the last years to end with a convergent effective field theory for nucleon-nucleon interactions including pions, for a review see e.g. [10]. On the one hand, we have the original Weinberg's proposal [5], with an undoubted phenomenological success [11]. Nevertheless, this scheme suffers from inconsistencies in the power counting due to the lack of higher order counterterms to absorb divergences generated by solving *numerically* the Lippmann-Schwinger equation so that a cut-off dependence remains in the resulting physical amplitudes. On the other hand, we have the Kaplan-Savage-Wise (KSW) effective field theory [18] with its consistent power counting that ends up with *analytical* nucleon-nucleon amplitudes. However, its phenomenological success and convergence [19] is just restricted to a very narrow region close to the nucleon-nucleon threshold despite having included explicitly the pion fields. This was clear from the analysis at NNLO in the KSW effective field theory performed in ref.[19] where the NNLO departs from data before the NLO and badly diverges for center-of-mass three-momentum above  $\sim 100$  MeV. The reason for this bad convergence properties were identified in the triplet channels with large contributions from the twice iterated pion exchange. That is, pions cannot be treated perturbatively in all the nucleon-nucleon channels and in particular in the  $S_1^3 - D_1^3$  one.

Hence, despite all the efforts made during the past years, the issue of deriving a consistent effective field theory for nucleon-nucleon interactions is still open. We perform in this paper a step forward by extending the range of convergence of the KSW amplitudes. In ref. [5] Weinberg proposed to calculate the nucleon-nucleon potential in a chiral expansion and then solve a Lippmann-Schwinger equation in order to avoid the large enhancements, due to factors  $2M/p$ , from the reducible two nucleon diagrams which do not enter in the calculation of the potential, see also ref.[8]. From a S-matrix point of view the Weinberg's proposal can be recasted so that one should resum the unitarity or right-hand cut, which is the responsible for all the unitarity bubbles with their large  $2M/p$  factors. Nevertheless, solving a Lippmann-Schwinger equation is not the only way to accomplish this and another one, more appropriate for quantum field theory can be established. In this way, one avoids the non trivial problems associated with the renormalization of a Lippmann-Schwinger equation with highly singular potentials at the origin as those coming from present effective field theories.

We propose here a general scheme to resum the unitarity cut. This scheme, originally motivated as an application of the N/D method [12, 13], was already employed in meson-meson [13, 14] and meson-baryon [15, 16] systems. This method should not be confused with Paddè resummations like those performed in the meson-meson or meson-baryon sectors [17]. Nevertheless, there are specific facts in the nucleon-nucleon scattering, associated with the largeness of the scattering lengths in the S-waves, that require a special treatment not present in any meson-meson or meson-nucleon system, as we explain below. In fact, a very reassuring feature of nucleon-nucleon physics is that non-perturbative physics manifests at very low center of mass three-momentum,  $p$ , as indicated by the presence of bound states and poles in unphysical sheets just below threshold. Hence, one can really establish a power counting since the nucleon-nucleon three-momentum is a small parameter and at the same type use non-perturbative techniques, as those to be used here to resum the right hand cut, within an under control expansion. It is also worth stressing that all the formalism presented here is analytic.

The paper is organized as follows. In sec.2 the novel formalism contained in this work is settled. This makes use of the KSW power counting and the reader unfamiliar with such power counting is referred to the original literature, refs.[18, 19]. It is shown how the unitarity cut can be easily resummed in terms of the inverse of a partial wave amplitude and how to perform a matching to the pure KSW amplitudes in order to fix an interacting kernel denoted by  $\mathcal{R}$ . Once this is done, we discuss in sec.3 the phenomenology and compare with data. Since all the expressions are analytic we fix many of the counterterms in terms of the Effective Range Expansion (ERE) parameters  $a_s$  and  $r_0$  in the S-waves order by order in the expansion. The agreement with data for the S-waves and the mixing angle  $S_1^3 - D_1^3$  is quite impressive in a broad energy range,  $p \lesssim 400$  MeV ( $T_{lab} \lesssim 360$  MeV), involving all the data points of the Nijmegen partial wave analysis [20]. Higher partial waves are also analyzed at the same order. However, only one pion exchange and the reducible part of twice iterated one pion exchange enter in the corresponding KSW amplitudes at this order. The results, which are very similar to those of the Weinberg's scheme at the corresponding order (LO in this case) [11], indicate that higher order corrections should be included so as to perform a more complete analysis for the  $P$  and  $D$  partial waves. We end with some conclusions.

## 2 Formalism

It seems that pions cannot be treated perturbatively. This is indeed the main reason for the failure of convergence of the KSW scheme, which considers pions perturbatively, in the nucleon-nucleon interactions for center of mass three-momentum  $p \lesssim 100$  MeV. This was clearly established in ref.[19], as one can see when comparing the calculated mixing parameter  $\epsilon_1$  at NLO [18] and NNLO [19]. While for very low momentum the NNLO calculations agree better with data, unfortunately for momenta higher than 100 MeV the NNLO calculations badly diverge from experiment, much more than the NLO results, and no improvement is obtained despite pions are explicitly included. This should be compared with the phenomenological success of the Weinberg's scheme in [6] and particularly in [11], where the chiral expansion seems to be under control, at least at the level of the phenomenology. In the latter scheme there are still the issues of avoiding cut-off dependence and the associated inconsistencies in the Weinberg's power counting that were established in refs.[8, 18].

In this paper we make use of the KSW amplitudes which are calculated within an effective field theory and are properly renormalized. There is nonetheless a clear difference between the KSW effective field theory and CHPT. While the latter is convergent in the  $SU(2)$  sector in an energy window that could be expected from the scales that are involved in the problem, the same does not occur with the former [19].

We want to include pions non-perturbatively but keeping at the same time the advantages of the KSW scheme that make it a true effective field theory. In order to accomplish this, we resum the right hand cut or unitarity cut so as to take care of the large  $2M/p$  factors from the two nucleon reducible diagrams [5]. This is also performed when solving a Lippmann-Schwinger equation, as originally proposed in ref.[5], but we will do it in a different fashion considering unitarity and analyticity in the form of a dispersion relation of the inverse of a partial wave.

Let us denote a partial wave by  $T_{L_J^{2S+1}, \hat{L}_J^{2S+1}}$ , where  $L$  and  $\hat{L}$  refer to the orbital angular momentum of the initial and final state respectively, and  $S$  and  $J$  indicate the total spin and total angular momentum of the systems, in order. Then unitarity requires above the nucleon-nucleon threshold and below the  $NN\pi$  one, which is around  $p \simeq 280$  MeV:

$$\text{Im}T_{L_J^{2S+1}, \hat{L}_J^{2S+1}} = \frac{Mp}{4\pi} \sum_{\ell} T_{L_J^{2S+1}, \ell_J^{2S+1}} (T_{\ell_J^{2S+1}, \hat{L}_J^{2S+1}})^* , \quad (2.1)$$

where  $M$  is the nucleon mass. It is easy to derive from the previous equation:

$$\text{Im} (T^{(2S+1)J})_{ij}^{-1} = -\frac{Mp}{4\pi} \delta_{ij} , \quad (2.2)$$

where  $T^{(2S+1)J}$  is a matrix whose matrix elements are those triplet partial waves that mix each other, e.g. for  $S_1^3 - D_1^3$  one has  $T_{11}^{31} = T_{S_1^3, S_1^3}$ ,  $T_{12}^{31} = T_{21}^{31} = T_{S_1^3, D_1^3}$  and  $T_{22}^{31} = T_{D_1^3, D_1^3}$ . In the previous equation we denote by  $(T^{(2S+1)J})^{-1}$  the inverse of the  $T^{(2S+1)J}$  matrix. If the partial waves do not mix then  $T^{(2S+1)J}$  is just a number equal to  $T_{L_J^{2S+1}, L_J^{2S+1}}$ . The imaginary part in the previous equation is the responsible for the unitarity cut. Thinking of a dispersion relation for the inverse of the amplitude this cut can be easily taken into account from eq.(2.2), as we previously did in the meson-meson [13] and meson-baryon [15, 16] sectors, and gives rise to the integral:

$$g_i(s) = \frac{1}{\pi} \int_{4M^2}^{\infty} \frac{Mp(s')}{4\pi} \frac{1}{s' - s + i0^+} ds' , \quad (2.3)$$

where  $s$  is the usual Mandelstam variable. This integral is divergent and requires a subtraction,  $M\nu_i/4\pi$ :

$$g_i(s) = \frac{M}{4\pi} \left( \nu_i + ip + \frac{M\sigma(s)}{\pi} \log \frac{1 - \sigma(s)}{1 + \sigma(s)} \right) , \quad (2.4)$$

with  $\sigma(s) = \sqrt{1 - \frac{4M^2}{s}}$ . In the physical region the logarithm is purely real and just gives rise to non-relativistic corrections that are derived by an analogous expression to eq.(2.3) but with  $Mp(s')/4\pi$  replaced by the relativistic phase space  $M^2 p(s')/2\pi\sqrt{s}$  in the integrand. Since we want to match with the KSW amplitudes, that absorb all the relativistic corrections in the vertices, the non-relativistic phase space factor  $Mp/4\pi$  is used as explicit source of imaginary part in eq.(2.4). The non-relativistic corrections from the logarithm of eq.(2.4) are essentially negligible in the energy range that we consider. Once this is done, one can write for the full partial wave matrix or number  $T^{(2S+1)J}$  the expression:

$$T^{(2S+1)J} = -[\mathcal{R}^{-1} + g]^{-1} . \quad (2.5)$$

In this expression all the other possible cuts of a nucleon-nucleon partial wave, either due to the exchange of other particles or because its helicity structure, are included in the input or kernel  $\mathcal{R}$  that we still must fix. The unitarity requirements, resummation of the infinite set of reducible diagrams with two intermediate nucleons, are accomplished by  $g(s)$ , which as stated is a diagonal matrix in the case of mixed partial waves, or just one function for the unmixed ones. E.g., in the coupled partial waves  $S_1^3$  and  $D_1^3$ ,  $g_{11}(s) = g_1(s)$  and corresponds to the  $S_1^3$  channel and  $g_{22}(s) = g_2(s)$  and refers to the  $D_1^3$  channel. Of course,  $g_{12}(s) = g_{21}(s) = 0$ .

We now specify  $\mathcal{R}$  in the key expression eq.(2.5). For that purpose we make use of the results of the KSW effective field theory for two nucleon systems and of its power counting, that we apply to  $\mathcal{R}$  and  $g$  in eq.(2.5). The matching procedure can be done for any given order in the calculation of the KSW amplitudes and for any subtraction constants  $\nu_i$  in  $g_i(s)$ . Once we determine the chiral expansion<sup>#2</sup> of  $\mathcal{R}$  and  $g$  we will match with the inverses of the KSW amplitudes order by order.

An important point is to establish the chiral order of  $g_i(s)$ . For the S-waves  $S_0^1$  and  $S_1^3$ , the corresponding elastic KSW amplitudes start at order  $p^{-1}$  and hence their inverses begin at order  $p$ . Thus one could think that  $g(s)$  should be order  $p$  as well, since this is the first order that appear in the inverses of the

<sup>#2</sup>As an abuse of language we also talk about a chiral expansion when considering the KSW power counting although, in this case,  $1/a$  is counted as order  $p$  and is not accounted for by one power of  $m_\pi$  [8, 18].

leading KSW partial waves. Would this be the case, then  $\mathcal{R}$  would also start at order  $p$ . If we continue along these lines the resulting phenomenology is not good and there is no clear improvement with regard to the problematic of the KSW calculations at NNLO. If, on the other hand, we think of higher partial waves, e.g.  $P$  and  $D$ , then we realize that the KSW amplitudes start at order  $p^0$  so that taking  $g$  and  $\mathcal{R}$  as order  $p^0$  is quite natural. If we take this option as well for the S-waves, and systematically derive the  $\mathcal{R}$  matrix elements by matching with the KSW inverse amplitudes, we will see below that the improvement with respect to the pure KSW scheme is quite impressive. Indeed, in order to match with the inverses of the KSW S-wave amplitudes, that start at order  $p$ , we must cancel exactly the order  $p^0$  contributions in these partial waves stemming from the ones of  $\mathcal{R}$  and  $g$ . This fine tuning reminds of the one usually advocated to explain the large scattering lengths in the S-waves channels [5].

Let us now analyze carefully the elastic  $S_0^1$  channel within the previous scheme. After that we will present more briefly the analogous procedure in the  $S_1^3 - D_1^3$  coupled channel sector and for the  $P$ ,  $D$ ,  $F_2^2$  and  $G_3^3$  waves.

- $S_0^1$  elastic partial wave.

The KSW  $S_0^1$  partial wave,  $A_{S_0^1}^{KSW}$ , was calculated at NLO (order  $p^0$ ) in ref.[18] and then at NNLO (order  $p$ ) in ref.[19]. Let us indicate these partial waves by  $A_{-1}(p)$ ,  $A_0(p)$  and  $A_1(p)$ , where the subindex indicates the chiral order. In the same way we write:

$$\mathcal{R} = R_0 + R_1 + R_2 + R_3 + \mathcal{O}(p^4) , \quad (2.6)$$

and  $g(s) = M\nu/4\pi + iMp/4\pi - p^2/2\pi^2 + \mathcal{O}(p^4)$ . Then we must match:

$$\frac{1}{A_{S_0^1}^{KSW}} = \left( \frac{1}{A_{-1}} \right) - \left( \frac{A_0}{A_{-1}^2} \right) + \left( \frac{A_0^2 - A_1 A_{-1}}{A_{-1}^3} \right) + \mathcal{O}(p^4) , \quad (2.7)$$

with

$$\begin{aligned} - \left( \frac{1}{\mathcal{R}} + g \right) &= - \left( \frac{1}{R_0} + \frac{M\nu}{4\pi} \right) + \left( \frac{R_1}{R_0^2} - i \frac{Mp}{4\pi} \right) + \left( \frac{p^2}{2\pi^2} + \frac{R_0 R_2 - R_1^2}{R_0^3} \right) + \left( \frac{R_1^3 - 2R_0 R_1 R_2 + R_0^2 R_3}{R_0^4} \right) \\ &+ \mathcal{O}(p^4) , \end{aligned} \quad (2.8)$$

where we have shown between brackets the different orders, from order  $p^0$  up to order  $p^3$ . As a result of the matching we can fix the different  $R_0$ ,  $R_1$ ,  $R_2$  and  $R_3$  in terms of  $\nu$ ,  $A_{-1}(p)$ ,  $A_0(p)$  and  $A_1(p)$ . We follow ref.[19], so that any of the previous amplitudes are scale independent at each order in the expansion.

Taking into account that

$$A_{-1} = - \frac{4\pi}{M} \frac{1}{\gamma + ip} , \quad (2.9)$$

following the notation of ref.[19], where  $\gamma$  is a quantity of order  $p$ , we can write the following expressions for the  $R_i$ :

$$\begin{aligned} R_0 &= - \frac{4\pi}{M\nu} , \\ R_1 &= - \frac{4\gamma\pi}{M\nu^2} , \\ R_2 &= - \frac{4(2\nu p^2 + \gamma^2 M\pi) + \nu(\frac{4\pi}{A_{-1}})^2 A_0(p)}{M^2 \nu^3} , \end{aligned}$$

$$\begin{aligned}
R_3 &= -\frac{1}{4M^2\nu^4\pi} \left( 8\gamma\nu \left( \frac{4\pi}{A_{-1}} \right)^2 \pi A_0(p) - \nu^2 \left( \frac{4\pi}{A_{-1}} \right)^3 A_0(p)^2 + 4\pi [4\gamma(4\nu p^2 + \gamma^2 M\pi) \right. \\
&\quad \left. + \nu^2 \left( \frac{4\pi}{A_{-1}} \right)^2 A_1(p)] \right) . \tag{2.10}
\end{aligned}$$

Hence working at NLO in the KSW amplitudes [18] we will have,

$$\mathcal{R}^{NLO} = R_0 + R_1 + R_2 , \tag{2.11}$$

and matching with the ones at NNLO [19]:

$$\mathcal{R}^{NNLO} = R_0 + R_1 + R_2 + R_3 . \tag{2.12}$$

The resulting  $\mathcal{R}$  is substituted in eq.(2.5) and in this way we calculate the partial waves at the different orders considered so forth. It is clear that the process above can be done so as to match with a KSW amplitude calculated at any order. In this way the precision of the resulting amplitude is increased order by order. In the pionless effective field theory, where only local interactions and an even number of derivatives appear in the Lagrangians, the previous matching procedure is equivalent to solve a Lippmann-Schwinger equation but with the important remark that the  $\mathcal{R}$  contains only *renormalized* amplitudes and should then be compared with the renormalized on-shell potential. For a proof of this statement in the meson-meson sector, that can be translated straightforwardly to the pionless effective field theory case, see ref.[13].

- $S_1^3 - D_1^3$  coupled partial waves.

In this case  $\mathcal{R}$  is a  $2 \times 2$  symmetric matrix:

$$\mathcal{R} = \begin{pmatrix} R_{11} & R_{12} \\ R_{12} & R_{22} \end{pmatrix} , \tag{2.13}$$

and  $g(s) = \text{diagonal}(g_1(s), g_2(s))$  with its associated subtraction constants  $\nu_1$  and  $\nu_2$ . Like in the  $S_0^1$  channel we will make  $g_1 = \mathcal{O}(p^0)$  and  $R_{11} = R_{11,0} + R_{11,1} + R_{11,2} + R_{11,3} + \mathcal{O}(p^4)$ . In the KSW scheme at the leading order the  $S_1^3$  and  $D_1^3$  are uncoupled and the mixing starts at NLO. In order to keep this sequence of facts in our amplitudes, we consider  $R_{12} = R_{12,1} + R_{12,2} + \mathcal{O}(p^3)$ . Finally, since the  $D_1^3$  partial wave starts at order  $p^0$  we take  $R_{22} = R_{22,0} + R_{22,1} + \mathcal{O}(p^2)$ .

The resulting expressions to match between are the expansions of the matrix elements of the inverse of the KSW matrix of partial waves for the  $S_1^3 - D_1^3$  sector,  $A_{S_1^3 - D_1^3}^{KSW}$ :

$$\begin{aligned}
(A_{S_1^3 - D_1^3}^{KSW})_{11}^{-1} &= \left( \frac{1}{A_{11,-1}} \right) + \left( \frac{A_{12,0}^2 - A_{11,0}A_{22,0}}{A_{11,-1}^2 A_{22,0}} \right) \\
&+ \left( \frac{A_{12,0}^4 + 2A_{11,-1}A_{12,0}A_{12,1}A_{22,0} + (A_{11,0}^2 - A_{11,-1}A_{11,1})A_{22,0}^2}{A_{11,-1}^3 A_{22,0}^2} \right. \\
&\quad \left. - \frac{A_{12,0}^2(2A_{11,0}A_{22,0} + A_{11,-1}A_{22,1})}{A_{11,-1}^3 A_{22,0}^2} \right) + \mathcal{O}(p^4) , \\
(A_{S_1^3 - D_1^3}^{KSW})_{12}^{-1} &= - \left( \frac{A_{12,0}}{A_{11,-1}A_{22,0}} \right) - \left( \frac{A_{12,0}^3 + A_{11,-1}A_{12,1}A_{22,0} - A_{12,0}(A_{11,0}A_{22,0} + A_{11,-1}A_{22,1})}{A_{11,-1}^2 A_{22,0}^2} \right) \\
&+ \mathcal{O}(p^3) , \\
(A_{S_1^3 - D_1^3}^{KSW})_{22}^{-1} &= \left( \frac{1}{A_{22,0}} \right) + \left( \frac{A_{12,0}^2 - A_{11,-1}A_{22,1}}{A_{11,-1}A_{22,0}^2} \right) + \mathcal{O}(p^2) , \tag{2.14}
\end{aligned}$$

and the ones that result from the expansion of eq.(2.5) with the counting for  $\mathcal{R}$  and  $g$  established above:

$$\begin{aligned}
(T^{31})_{11}^{-1} &= -\left(\frac{M\nu_1}{4\pi} + \frac{1}{R_{11,0}}\right) + \left(\frac{R_{11,1}}{R_{11,0}^2} - i\frac{Mp}{4\pi}\right) + \left(\frac{p^2}{2\pi^2} + \frac{R_{11,0}R_{11,2}R_{22,0} - R_{11,1}^2R_{22,0} - R_{11,0}R_{12,1}^2}{R_{11,0}^3R_{22,0}}\right) \\
&- \left(\frac{-R_{11,1}^3R_{22,0}^2 + 2R_{11,0}R_{11,1}R_{22,0}(-R_{12,1}^2 + R_{11,2}R_{22,0})}{R_{11,0}^4R_{22,0}^2}\right. \\
&\left.- \frac{R_{11,0}^2(-2R_{12,1}R_{12,2}R_{22,0} + R_{11,3}R_{22,0}^2 + R_{12,1}^2R_{22,1})}{R_{11,0}^4R_{22,0}^2}\right) + \mathcal{O}(p^4), \\
(T^{31})_{12}^{-1} &= \left(\frac{R_{12,1}}{R_{11,0}R_{22,0}}\right) - \left(\frac{R_{11,1}R_{12,1}R_{22,0} - R_{11,0}R_{12,2}R_{22,0} + R_{11,0}R_{12,1}R_{22,1}}{R_{11,0}^2R_{22,0}^2}\right) + \mathcal{O}(p^3), \\
(T^{31})_{22}^{-1} &= -\left(\frac{M\nu_2}{4\pi} + \frac{1}{R_{22,0}}\right) + \left(\frac{R_{22,1}}{R_{22,0}^2} - i\frac{Mp}{4\pi}\right) + \mathcal{O}(p^2). \tag{2.15}
\end{aligned}$$

We can then easily solve for the  $R_{ij,k}$  and we obtain:

$$\begin{aligned}
R_{11,0} &= -\frac{4\pi}{M\nu_1}, \\
R_{11,1} &= -\frac{4\gamma\pi}{M\nu_1^2}, \\
R_{11,2} &= \frac{1}{M^2\nu_1^3(4\pi + M\nu_2A_{22,0})} \{ M^3\nu_1\nu_2(\gamma + ip)^2A_{12,0}^2 - 4(2\nu_1p^2 + \gamma^2M\pi)(4\pi + M\nu_2A_{22,0}) \\
&- M^2\nu_1(\gamma + ip)^2A_{11,0}(4\pi + M\nu_2A_{22,0}) \}, \\
R_{11,3} &= \frac{1}{4M\nu_1^2\pi A_{22,0}^2} \{ -M(\gamma + ip)^2(M(\gamma + ip)A_{12,0}^4 - 8\pi A_{12,0}A_{12,1}A_{22,0} + (M(\gamma + ip)A_{11,0}^2 \\
&+ 4\pi A_{11,1})A_{22,0}^2 - 2A_{12,0}^2(M(\gamma + ip)A_{11,0}A_{22,0} - 2\pi A_{22,1})) + \frac{1}{\nu_1^2(4\pi + M\nu_2A_{22,0})^2} ( \\
&\times 8\pi(2\gamma^3\pi A_{22,0}^2(4\pi + M\nu_2A_{22,0})^2 - \frac{1}{M}(\gamma A_{22,0}(4\pi + M\nu_2A_{22,0})^2(-M^2\nu_1(\gamma + ip)^2A_{12,0}^2 \\
&+ (4(2\nu_1p^2 + \gamma^2M\pi) + M^2\nu_1(\gamma + ip)^2A_{11,0})A_{22,0})) - M\nu_1(\gamma + ip)^2A_{12,0}(-M\nu_1(\gamma + ip)A_{12,0}^3 \\
&\times (2\pi + M\nu_2A_{22,0}) + 4\nu_1\pi A_{12,1}A_{22,0}(4\pi + M\nu_2A_{22,0}) + A_{12,0}(M(4\gamma\nu_2\pi - 2i\nu_1p\pi \\
&+ M\nu_1\nu_2(\gamma + ip)A_{11,0})A_{22,0}^2 - 8\nu_1\pi^2A_{22,1} + 4\pi A_{22,0}(4\gamma\pi + M\nu_1(\gamma + ip)A_{11,0} \\
&- M\nu_1\nu_2A_{22,1})))) \}, \\
R_{12,1} &= \frac{4(\gamma + ip)\pi A_{12,0}}{\nu_1(4\pi + M\nu_2A_{22,0})}, \\
R_{12,2} &= \frac{1}{\nu_1^2(4\pi + M\nu_2A_{22,0})^2} \{ (\gamma + ip)(-M^2\nu_1\nu_2(\gamma + ip)A_{12,0}^3 + 4\nu_1\pi A_{12,1}(4\pi + M\nu_2A_{22,0}) \\
&+ A_{12,0}(M\nu_1(\gamma + ip)A_{11,0}(4\pi + M\nu_2A_{22,0}) + 4\pi(4\gamma\pi + M(\gamma\nu_2 - i\nu_1p)A_{22,0} - M\nu_1\nu_2A_{22,1}))) \}, \\
R_{22,0} &= -\frac{4\pi A_{22,0}}{4\pi + M\nu_2A_{22,0}}, \\
R_{22,1} &= -\frac{4\pi(M(\gamma + ip)A_{12,0}^2 - iMpA_{22,0}^2 + 4\pi A_{22,1})}{(4\pi + M\nu_2A_{22,0})^2}. \tag{2.16}
\end{aligned}$$

Similarly as in the  $S_0^1$  case, working at NLO implies:

$$\begin{aligned} R_{11}^{NLO} &= R_{11,0} + R_{11,1} + R_{11,2} , \\ R_{12}^{NLO} &= R_{12,1} , \\ R_{22}^{NLO} &= R_{22,0} , \end{aligned} \quad (2.17)$$

and at NNLO:

$$\begin{aligned} R_{11}^{NNLO} &= R_{11,0} + R_{11,1} + R_{11,2} + R_{11,3} , \\ R_{12}^{NNLO} &= R_{12,1} + R_{12,2} , \\ R_{22}^{NNLO} &= R_{22,0} + R_{22,1} . \end{aligned} \quad (2.18)$$

- $P$ ,  $D$ ,  $F_2^3$  and  $G_3^3$  partial waves except  $D_1^3$ .

For the  $P$  and  $D$  waves, the NLO KSW amplitudes [18] just contain one pion exchange and at NNLO [19, 21] they only include in addition the reducible part of the twice iterated one pion exchange. The physics behind this is then quite limited and this will show up in the phenomenology which, on the other hand, is of the same quality as that of the LO Weinberg's power counting scheme results, ref.[11], which contain a similar input for the potential. For these partial waves we follow the same kind of treatment as discussed above. For the elastic ones we have  $\mathcal{R} = R_0 + R_1 + \mathcal{O}(p^2)$  and  $g = \mathcal{O}(p^0)$  and for the coupled channel partial waves, namely  $P_2^3 - F_2^3$  and  $D_3^3 - G_3^3$ , the treatment will be similar to that of the  $S_1^3 - D_1^3$  case, though here, we will take  $R_{ij} = R_{ij,0} + R_{ij,1} + \mathcal{O}(p^2)$  and  $g_i(s) = \mathcal{O}(p^0)$ , since all the channels start to contribute at the same order  $p^0$ .

For the elastic case, after performing the appropriate chiral expansion and matching with the inverse of the KSW amplitude, as done previously, one can write:

$$\begin{aligned} R_0 &= -\frac{A_0}{1 + A_0 \frac{M\nu}{4\pi}} , \\ R_1 &= -\frac{1}{(1 + A_0 \frac{M\nu}{4\pi})^2} (A_1 - i \frac{pM}{4\pi} A_0^2) , \end{aligned} \quad (2.19)$$

so that,

$$\begin{aligned} \mathcal{R}^{NLO} &= R_0 , \\ \mathcal{R}^{NNLO} &= R_0 + R_1 . \end{aligned} \quad (2.20)$$

For the two coupled channel partial waves one performs the chiral expansion in coupled channels. Taking into account the remarks in the last paragraph, one easily obtains:

$$\begin{aligned} R_{11,0} &= -\frac{4\pi(4\pi A_{11,0} - M\nu_2 A_{12,0}^2 + M\nu_2 A_{11,0} A_{22,0})}{(4\pi + M\nu_1 A_{11,0})(4\pi + M\nu_2 A_{22,0}) - M^2 \nu_1 \nu_2 A_{12,0}^2} , \\ R_{11,1} &= \frac{1}{\left[M^2 \nu_1 \nu_2 A_{12,0}^2 - (4\pi + M\nu_1 A_{11,0})(4\pi + M\nu_2 A_{22,0})\right]^2} \left\{ 4i\pi(4i\pi A_{11,1}(4\pi + M\nu_2 A_{22,0})^2 \right. \\ &+ M(M^2 \nu_2^2 p A_{12,0}^4 - 8i\nu_2 \pi A_{12,1} A_{12,0}(4\pi + M\nu_2 A_{22,0}) + p A_{11,0}^2 (4\pi + M\nu_2 A_{22,0})^2 \\ &\left. - 2A_{12,0}^2 (-2iM\nu_2^2 \pi A_{22,1} + p(4\pi(-2\pi + M\nu_2 A_{11,0}) + M^2 \nu_2^2 A_{11,0} A_{22,0}))) \right\} , \end{aligned}$$

$$\begin{aligned}
R_{12,0} &= -\frac{16\pi^2 A_{12,0}}{(4\pi + M\nu_1 A_{11,0})(4\pi + M\nu_2 A_{22,0}) - M^2 \nu_1 \nu_2 A_{12,0}^2}, \\
R_{12,1} &= -\frac{1}{\left[M^2 \nu_1 \nu_2 A_{12,0}^2 - (4\pi + M\nu_1 A_{11,0})(4\pi + M\nu_2 A_{22,0})\right]^2} \left\{ 16\pi^2 (A_{12,1} (M^2 \nu_1 \nu_2 A_{12,0}^2 \right. \\
&+ (4\pi + M\nu_1 A_{11,0})(4\pi + M\nu_2 A_{22,0})) + iMA_{12,0}(-4p\pi A_{11,0} + M(\nu_1 + \nu_2)pA_{12,0}^2 + 4i\nu_2 \pi A_{22,1} \\
&+ iM\nu_1 \nu_2 A_{11,0} A_{22,1} - 4p\pi A_{22,0} - M\nu_1 p A_{11,0} A_{22,0} - M\nu_2 p A_{11,0} A_{22,0} \\
&+ i\nu_1 A_{22,1} (4\pi + M\nu_2 A_{22,0}))) \right\}, \\
R_{22,0} &= -\frac{4\pi(-M\nu_1 A_{12,0}^2 + (4\pi + M\nu_1 A_{11,0})A_{22,0})}{(4\pi + M\nu_1 A_{11,0})(4\pi + M\nu_2 A_{22,0}) - M^2 \nu_1 \nu_2 A_{12,0}^2}, \\
R_{22,1} &= \frac{1}{\left[M^2 \nu_1 \nu_2 A_{12,0}^2 - (4\pi + M\nu_1 A_{11,0})(4\pi + M\nu_2 A_{22,0})\right]^2} \left\{ 4i\pi(-8iM\nu_1 \pi (4\pi + M\nu_1 A_{11,0})A_{12,1} A_{12,0} \right. \\
&+ M^3 \nu_1^2 p A_{12,0}^4 + (4\pi + M\nu_1 A_{11,0})^2 (4i\pi A_{22,1} + M p A_{22,0}^2) - 2MA_{12,0}^2 (-2iM\nu_1^2 \pi A_{11,1} \\
&+ p(-8\pi^2 + M\nu_1 (4\pi + M\nu_1 A_{11,0}) A_{22,0}))) \right\}. \tag{2.21}
\end{aligned}$$

where the subindex 1 before the period always refers to the channel with lower orbital angular momentum and 2 to the highest one.

Working at NLO implies taking:

$$\begin{aligned}
R_{11}^{NLO} &= R_{11,0}, \\
R_{12}^{NLO} &= R_{12,0}, \\
R_{22}^{NLO} &= R_{22,0}, \tag{2.22}
\end{aligned}$$

and at NNLO:

$$\begin{aligned}
R_{11}^{NNLO} &= R_{11,0} + R_{11,1}, \\
R_{12}^{NNLO} &= R_{12,0} + R_{12,1}, \\
R_{22}^{NNLO} &= R_{22,0} + R_{22,1}. \tag{2.23}
\end{aligned}$$

We have checked that all the previous expressions give rise to a real  $\mathcal{R}$  in the physical nucleon-nucleon region with the correct KSW order for all the channels.

### 3 Results and discussion

In this section we consider the phenomenological applications of the previous scheme to the S and higher partial waves. Of particular relevance is to study the triplet S-wave channel,  $S_1^3$ , and its mixing with the  $D_1^3$ , since here the KSW amplitudes do not converge for  $p \lesssim 100$  MeV although pions are explicitly included. We first discuss the  $S_0^1$  channel and then consider the  $S_1^3$  coupled with the  $D_1^3$  partial wave. After that we turn to discuss the  $P$ ,  $D$ ,  $F_2^3$  and  $G_3^3$  waves and compare with other approaches.

- $S_0^1$  channel.

We follow the notation of ref.[19]. At NLO we have two counterterms,  $\xi_1$  and  $\xi_2$  together with  $\gamma$  which already appears at LO. The first two counterterms are calculated in terms of  $\gamma$  and the

scattering length  $a_s$  and effective range  $r_0$  by performing the effective range expansion in eq.(2.5) with  $\mathcal{R}^{NLO}$  given in eq.(2.11). We then have:

$$\begin{aligned}\xi_1 &= \frac{-g_A^2 M^2 (6\gamma^2 - 8\gamma m_\pi + 3m_\pi^2)(-1 + a_s\nu)^2 + 12f^2 m_\pi^2 (4 - 8a_s\nu + a_s^2 M \nu^2 \pi r_0)}{96f^2 m_\pi^2 (-1 + a_s\nu)^2 \pi^2}, \\ \xi_2 &= \frac{M(g_A^2 \gamma M(\gamma - 2m_\pi)\nu(-1 + a_s\nu) + 8f^2(-\nu^2 + \gamma^2(-1 + a_s\nu) + \gamma\nu(-1 + a_s\nu))\pi)}{32f^2 m_\pi^2 \nu(-1 + a_s\nu)\pi^2}.\end{aligned}\quad (3.1)$$

At NNLO there are other counterterms,  $\xi_3$ ,  $\xi_4$  and  $\xi_5$ . The KSW power counting implies that  $\xi_5$  must be small. We either fix it to zero or leave it as a free parameter in the fits, turning out to be negligibly small in this case. So that in the following we take  $\xi_5 = 0$  in this channel. The counterterms  $\xi_3$  and  $\xi_4$  are then fixed in terms of  $\xi_1$ ,  $\xi_2$ ,  $\gamma$ ,  $a_s$  and  $r_0$  by performing the ERE. At NNLO we perform two kind of fits, either  $\xi_1$  and  $\xi_2$  are free parameters or they are fixed once again by the NLO expression, eq.(3.1), in the fitting procedure. The expressions of  $\xi_4$  and  $\xi_3$  in terms of  $\xi_1$ ,  $\xi_2$ ,  $\gamma$ ,  $a_s$  and  $r_0$  are:

$$\begin{aligned}\xi_3 &= \frac{1}{1536f^4 m_\pi^2 \nu^2 (-1 + a_s\nu)\pi^3} \{ 48f^2 g_A^2 M \nu (-1 + a_s\nu) \pi (2\gamma^3 M + \gamma^2 M (-4m_\pi + \nu) + 8m_\pi^3 \nu \pi \xi_2 \\ &\quad - 2\gamma m_\pi \nu (M + 4m_\pi \pi \xi_2)) - 384f^4 \pi^2 (\gamma^2 M \nu (1 - a_s\nu) + \gamma^3 (M - a_s M \nu) - \gamma \nu (-1 + a_s\nu) \\ &\quad \times (M \nu - 8m_\pi^2 \pi \xi_2) + \nu^2 (M \nu + 4m_\pi^2 (-1 + a_s\nu) \pi \xi_2)) + g_A^4 M^3 \nu^2 (-1 + a_s\nu) (6\gamma^3 - 21\gamma^2 m_\pi \\ &\quad - \gamma m_\pi^2 (-18 + \log(4096)) + m_\pi^3 \log(4096)) \} , \\ \xi_4 &= -\frac{1}{3072f^4 m_\pi^2 \nu (-1 + a_s\nu)^2 \pi^3} \{ 384f^4 m_\pi^2 \pi (8\gamma (-1 + a_s\nu)^2 (-1 + 2\pi^2 \xi_1) + \nu (-4 + 8\pi^2 \xi_1 \\ &\quad + a_s^2 \nu^2 \pi (-Mr_0 + 8\pi \xi_1) + 8a_s \nu (1 - 2\pi^2 \xi_1))) + 32f^2 g_A^2 M (-1 + a_s\nu)^2 \pi (12\gamma^3 M + \gamma^2 M (-16m_\pi + 6\nu) \\ &\quad + 2\gamma m_\pi (M (3m_\pi - 4\nu) + 12m_\pi \nu \pi (\xi_1 - 2\xi_2)) + m_\pi^2 \nu (3M + 8m_\pi \pi (-3\xi_1 + 4\xi_2))) \\ &\quad + g_A^4 M^3 \nu (-1 + a_s\nu)^2 (48\gamma^3 - 135\gamma^2 m_\pi + 2m_\pi^3 (-13 + 4\log(16)) - 4\gamma m_\pi^2 (-27 + \log(4096))) \} .\end{aligned}\quad (3.2)$$

The dashed line in fig.1 represents the NLO fit from eq.(2.5). At NNLO we indicate by the dash-dotted line the fit with  $\xi_1$ ,  $\xi_2$  calculated as in NLO, so that only  $\nu$  enters as a free parameter in the fit. The solid line represents the NNLO fit leaving  $\xi_1$  and  $\xi_2$  as free parameters. We also show by the dotted line the NNLO KSW phase shifts from ref.[19]. The values for the parameters that we take are  $f = 130.673$  MeV,  $g_A = 1.267$ ,  $m_\pi = 138$  MeV,  $M = 939$  MeV,  $a_s = -23.714$  fm and  $r_0 = 2.73$  fm. On the other hand, since  $a_s$  is so large,  $\gamma$  can be taken directly zero and we do fix it in that way. We have made a least square minimization process since the errors from the Nijmegen partial wave analysis [20] are in general extremely small. Our NLO results are fitted up to  $p < 300$  MeV and the NNLO ones are fitted to the whole energy range,  $T_{lab} < 360$  MeV. In this channel the KSW scheme works quite well, as shown in the figure by the dotted line. In our scheme the NLO works worse than both NNLO results which fit the data up to rather high energies. We show in table 1 the fitted and calculated values for the parameters involved in this partial wave. The latter are indicated with a star in the resulting numerical value.

$S_0^1$	NLO	NNLO	NNLO
$\nu$	270 MeV	710 MeV	630 MeV
$\xi_1$	0.23*	0.24*	0.41
$\xi_2$	0.03*	0.03*	0.16
$\xi_3$	...	0.21*	0.20*
$\xi_4$	...	0.23*	0.07*

Table 1: Counterterms and subtraction constant in the  $S_0^1$  channel at NLO and NNLO. The stars indicate that the corresponding parameters have been calculated from the ERE in terms of the other ones,  $a_s$  and  $r_0$  as explained in the text.

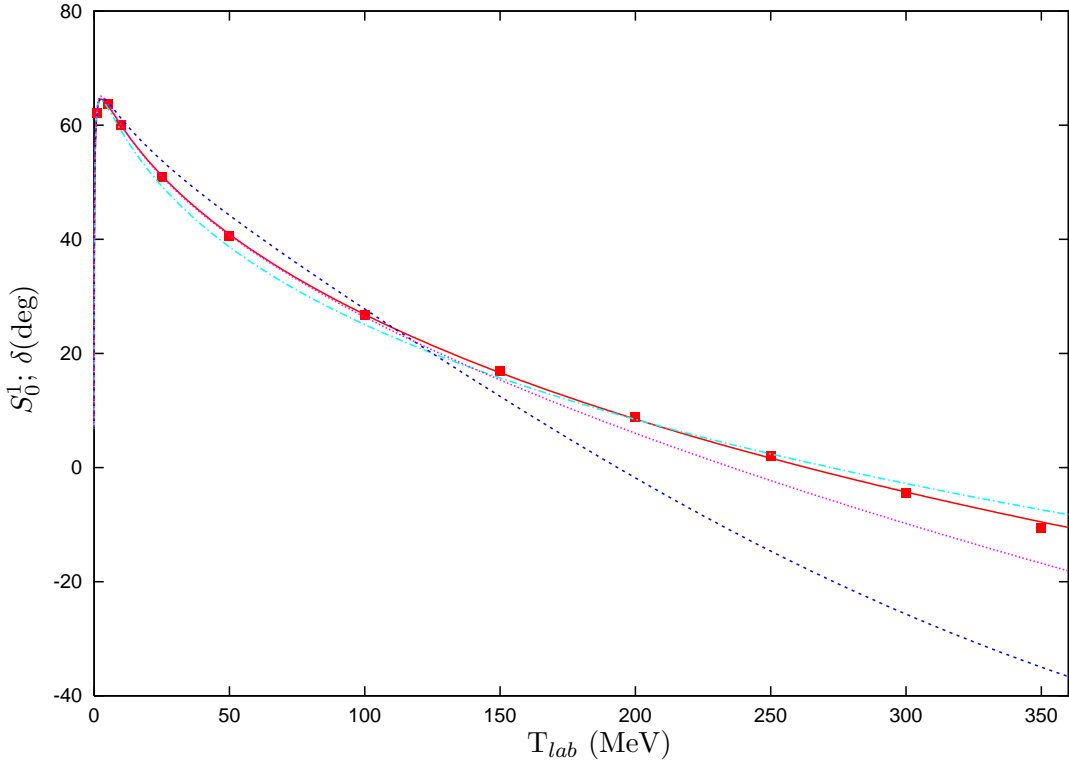


Figure 1: Phase shifts for the  $S_0^1$  channel. The dotted line is the NNLO KSW result [19]. The dashed line represents the NLO results from eq.(2.5). The dash-dotted and solid lines are the NNLO results with  $\xi_1$ ,  $\xi_2$  fixed as in NLO or taken as free parameters, respectively. The data correspond to the Nijmegen partial wave analysis, ref.[20].

- $S_1^3 - D_1^3$  coupled channels.

We treat the counterterms in analogous lines as described above for the  $S_0^1$  channel. Nevertheless, we keep now  $\gamma$  as a free parameter for the fit as well as  $\xi_5$  and  $\xi_6$  at NNLO. The  $\xi_6$  counterterm is a new one related to the  $S_1^3 - D_1^3$  mixing. One should take into account that although we use the same names for  $\gamma$  and the  $\xi$ 's counterterms as in the  $S_0^1$  case, they are indeed different [18, 19]. As before  $\xi_1$  and  $\xi_2$  are given at NLO in terms of  $\gamma$ ,  $a_s$  and  $r_0$  from the ERE. At NNLO we then calculate  $\xi_3$  and  $\xi_4$  from  $\xi_1$ ,  $\xi_2$ ,  $\gamma$ ,  $a_s$  and  $r_0$  with now  $\xi_1$  and  $\xi_2$  either taken as free parameters or

fixed as in NLO. The expressions for  $\xi_1$ ,  $\xi_2$ ,  $\xi_3$  and  $\xi_4$  determined from the ERE are the following:

$$\begin{aligned}
\xi_1 &= \frac{1}{96f^2m_\pi^2(-1+a_s\nu_1)^2\pi^2} \left\{ -g_A^2M^2(6\gamma^2 - 8\gamma m_\pi + 3m_\pi^2)(-1+a_s\nu_1)^2 + 12f^2m_\pi^2(4 - 8a_s\nu_1 \right. \\
&\quad \left. + a_s^2M\nu_1^2\pi r_0) \right\} , \\
\xi_2 &= \frac{1}{32f^2m_\pi^2\nu_1(-1+a_s\nu_1)\pi^2} \left\{ M(g_A^2\gamma M(\gamma - 2m_\pi)\nu_1(-1+a_s\nu_1) + 8f^2(-\nu_1^2 \right. \\
&\quad \left. + \gamma^2(-1+a_s\nu_1) + \gamma\nu_1(-1+a_s\nu_1))\pi) \right\} , \\
\xi_3 &= \frac{1}{2560f^4m_\pi^2\nu_1^2(-1+a_s\nu_1)\pi^3} \left\{ 80f^2g_A^2M\nu_1(-1+a_s\nu_1)\pi(2\gamma^3M + \gamma^2M(-4m_\pi + \nu_1) + 8m_\pi^3\nu_1\pi\xi_2 \right. \\
&\quad - 2\gamma m_\pi\nu_1(M + 4m_\pi\pi\xi_2)) - 640f^4\pi^2(\gamma^2M\nu_1(1 - a_s\nu_1) + \gamma^3(M - a_sM\nu_1) - \gamma\nu_1(-1 + a_s\nu_1) \right. \\
&\quad \times (M\nu_1 - 8m_\pi^2\pi\xi_2) + \nu_1^2(M\nu_1 + 4m_\pi^2(-1 + a_s\nu_1)\pi\xi_2)) + g_A^4M^3\nu_1^2(-1 + a_s\nu_1)(10\gamma^3 - 95\gamma^2m_\pi \right. \\
&\quad \left. - 5\gamma m_\pi^2(-15 + \log(4096)) + 2m_\pi^3(-8 + \log(67108864))) \right\} , \\
\xi_4 &= -\frac{1}{107520f^4m_\pi^2\nu_1(-1+a_s\nu_1)^2\pi^3} \left\{ 13440f^4m_\pi^2\pi(8\gamma(-1 + a_s\nu_1)^2(-1 + 2\pi^2\xi_1) + \nu_1(-4 + 8\pi^2\xi_1 \right. \\
&\quad + a_s^2\nu_1^2\pi(-Mr_0 + 8\pi\xi_1) + 8a_s\nu_1(1 - 2\pi^2\xi_1))) + 1120f^2g_A^2M(-1 + a_s\nu_1)^2\pi(12\gamma^3M + \gamma^2M(-16m_\pi \right. \\
&\quad + 6\nu_1) + 2\gamma m_\pi(M(3m_\pi - 4\nu_1) + 12m_\pi\nu_1\pi(\xi_1 - 2\xi_2)) + m_\pi^2\nu_1(3M + 8m_\pi\pi(-3\xi_1 + 4\xi_2))) \right. \\
&\quad + g_A^4M^3\nu_1(-1 + a_s\nu_1)^2(1680\gamma^3 - 3325\gamma^2m_\pi - 6m_\pi^3(913 + 1248\log(2) + 280\log(4) - 336\log(16) \right. \\
&\quad \left. - 140\log(256)) - 840\gamma m_\pi^2(-12 + \log(256))) \right\} . \tag{3.3}
\end{aligned}$$

The results of the fit are presented in figs.2 and 5. In fig.2 we show the phase shifts for the partial wave  $S_1^3$  and the mixing angle  $\epsilon_1$ . The latter is defined so that  $|S_{11}| = \cos(2\epsilon_1)$ . We take  $a_s = 5.425$  fm and  $r_0 = 1.749$  fm in the  $S_1^3$  channel. In fig.5 we present the elastic  $D_1^3$  phase shifts together with the phase shifts of the other D-waves. The  $\nu_1$  and  $\nu_2$  are subjected to rather large uncertainties from the fit. At NLO the symbol  $> \Lambda_{\chi PT}$  in table 2 indicates that at this order the subtractions constants  $\nu_i$  can take any value arbitrarily large, let us say, above the chiral symmetry breaking scale. At NNLO the value shown for  $\nu_1$  is indicative, the uncertainty being typically around 100 MeV and one can find other similar fits with  $\nu_1$  e.g. around 300 MeV. In addition, the minimization program can find other kind of minima with rather different values for the  $\xi_1 - \xi_4$  counterterms to those shown in the third column of table 2 and with  $\nu_1$  as large as  $M_\rho$ . Nevertheless, we have chosen the results shown in the third column of table 2 since they come up very similar to those from the more restricted fits of the first and second columns, and furthermore they drive to smaller corrections to  $R_{11}$  at NNLO when compared with its value at NLO, see fig.3.

The agreement with data of the new scheme presented here, as shown in figs.2, is remarkably good. At NLO, dashed-lines, the results already follow closely the trend of the data. At NNLO, we distinguish between two types of fits as in the  $S_0^1$  case. They are indicated by the dash-dotted lines, which correspond to the NNLO results when  $\xi_1$  and  $\xi_2$  obey eq.(3.3) from the ERE, and by the solid lines when the previous counterterms are taken as free parameters in the fit. Both curves are very similar and agree very well with data. As it is well known, the KSW approach treated in its standard form [19] presents serious problems of convergence, as it is apparent when considering the NNLO KSW results [19] given by the dotted line in fig.2. They only converge for very low energies although the pion fields are explicitly included. Particularly serious is the discrepancy with the mixing angle  $\epsilon_1$ . This observable has no counterterms at NLO KSW and only includes one free counterterm,  $\xi_6$ , at NNLO. Furthermore, it is free of the large cancellations that

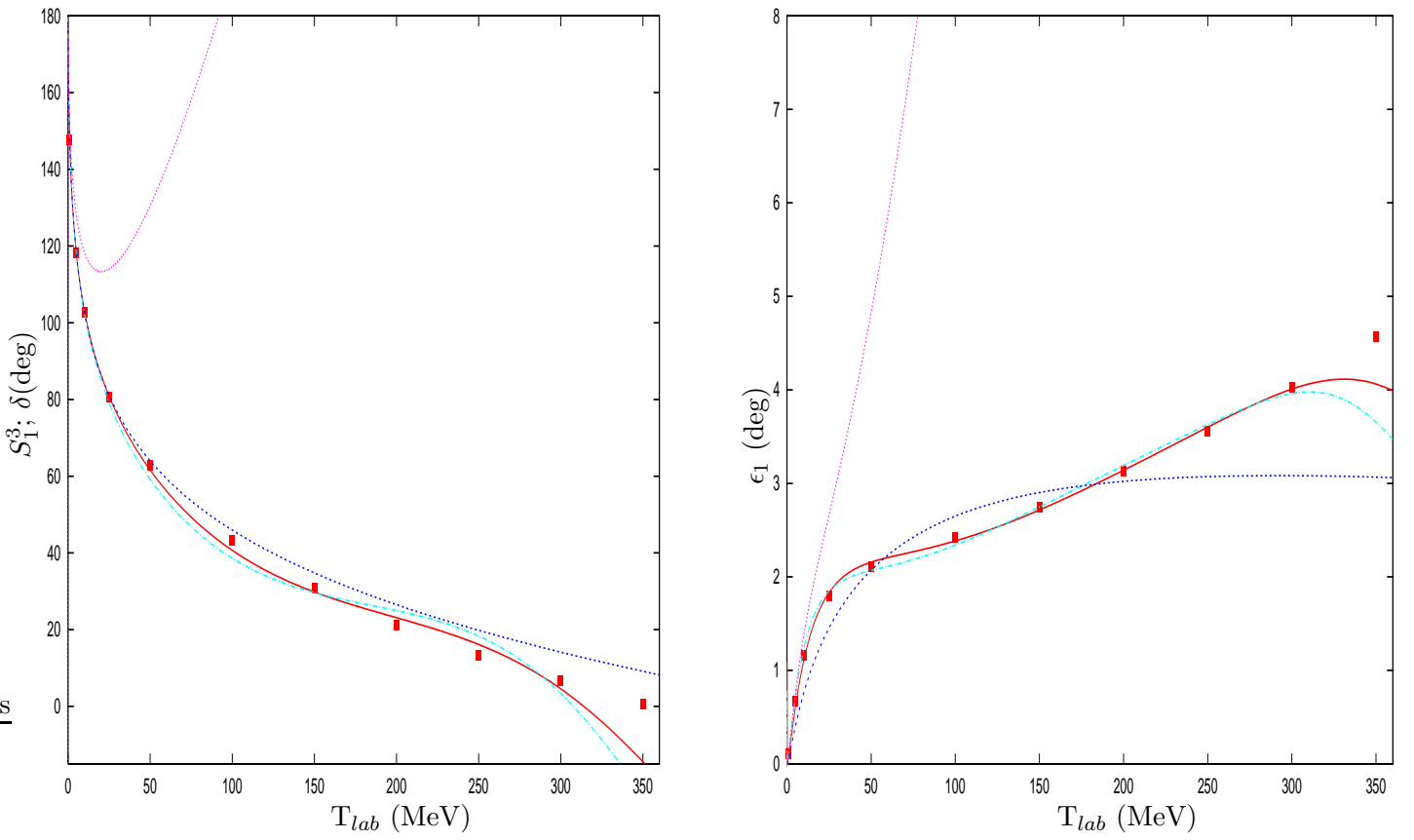


Figure 2: Phase shifts for the  $S_1^3$  channel and mixing angle  $\epsilon_1$ . The dotted line is the NNLO KSW result [19]. The dashed line represents the NLO results from eq.(2.5). The dash-dotted and solid lines are the NNLO results with  $\xi_1, \xi_2$  fixed as in NLO or taken as free parameters, respectively. The data correspond to the Nijmegen partial wave analysis, ref.[20].

affect  $\delta(S_1^3)$ . It was clarified in ref.[19] that his bad behaviour was due to large corrections from the twice iterated one pion exchange diagrams which are enhanced by large numerical factors. In our power counting the input kernel,  $\mathcal{R}$ , is infinitely iterated and with it the pion exchange as any other contribution. This ensures that pions are treated non perturbatively which is behind the phenomenological success of figs.2. Note that the proposal of Weinberg [5] of solving a Lippmann-Schwinger for calculating nucleon-nucleon scattering was motivated to avoid the large  $2M$  factors that reduce to  $M_\rho^2/2M \simeq \Lambda_{NN}$  the expansion scale for KSW NN effective field theory, which also appears in nuclear matter [22, 23]. Since the scale  $\Lambda_{NN}$  is already pretty low, if further numerical factors enhance higher order corrections, great disagreement with data can be expected giving rise to non-perturbative phenomena like in some of the triplet NN channels [19] within the KSW approach. In table 2 we show the fitted and calculated parameters at NLO and NNLO in our scheme. As in the  $S_0^1$  case the stars indicate that the corresponding values are calculated in terms of the ERE.

In the KSW power counting, when solving perturbatively the renormalization group equations one

$S_1^3, S_1^3 - D_1^3$	NLO	NNLO	NNLO
$\nu_1$	$> \Lambda_{\chi PT}$	170 MeV	190 MeV
$\nu_2$	$> \Lambda_{\chi PT}$	590 MeV	560 MeV
$\gamma$	$0.42 \text{ fm}^{-1}$	$0.39 \text{ fm}^{-1}$	$0.51 \text{ fm}^{-1}$
$\xi_1$	$0.31^*$	$0.47^*$	0.28
$\xi_2$	$-0.03^*$	$0.04^*$	0.06
$\xi_3$	...	$-0.01^*$	$-0.10^*$
$\xi_4$	...	$-0.08^*$	$-0.06^*$
$\xi_5$	...	0.17	0.17
$\xi_6$	...	0.62	0.47

Table 2: Counterterms and subtraction constants in the  $S_1^3, S_1^3 - D_1^3$  channels at NLO and NNLO. The stars indicate that the corresponding parameters have been calculated from the ERE in terms of the other ones,  $a_s$  and  $r_0$  as explained in the text.

has [19],

$$\xi_5 = \rho \frac{m_\pi^2 M}{4\pi} \quad (3.4)$$

and since  $\rho$  is order  $p^0$ , given by  $\Lambda_{NN}$ , then  $\xi_5$  is a quantity of order  $p^2$  and at NNLO, within the pure KSW scheme, can be fixed to zero [19] since it corresponds to higher orders. From the performed fits we have obtained that  $\xi_5$  is around 0.17. Taking  $\rho \propto \Lambda_{NN}^{-3}$ , and the proportionality constant around 1, from eq.(3.4) and the value of  $\xi_5$ , one calculates  $\Lambda_{NN} \simeq 200$  MeV, of the right order of magnitude, since  $M_\rho^2/2M(g_A^2) \simeq 300(200)$  MeV. Hence the fitted value of  $\xi_5$  is of a rather natural size. Because we are fitting data with eq.(2.5), that resums infinite orders from the original KSW amplitudes (we make a chiral expansion in  $\mathcal{R}$  and pions are treated non-perturbatively), one should take the counterterms that enter to a given order in the KSW amplitudes and fix them directly to data with eq.(2.5) in a broad energy regime rather than to stick to (pionic-)perturbative renormalization group results. In fact, all the resulting values for the  $\xi_i$  parameters given in tables 1 and 2 are of natural size within the pure KSW scheme, that is a fraction of 1 [19, 18]. This is the important point for us since with this natural sized counterterms we may consider the KSW amplitudes well behaved in the very narrow energy region around threshold where KSW amplitudes work and can be used in the matching process with eq.(2.5).

We also show in fig.3 the absolute values  $|\mathcal{R}^{NLO}|$  and  $|\mathcal{R}^{NNLO}|$  for the  $S_0^1$  channel (solid lines) and the same, although divided by four to keep the lines on the same scale, for the matrix element  $|R_{11}|$  of the  $S_1^3$  channel. The thick lines refer to the NNLO calculations and the thin ones to NLO. The convergence properties are quite good in a broad range of center of mass three momentum  $p$  as is apparent in this figure.

- $P, D, F_2^3$  and  $G_3^3$  partial waves.

Up to NNLO in the KSW approach, order  $p$ , the physics included in the description of partial waves higher than  $S$  waves, except for the mixing between the  $S_1^3 - D_1^3$ , contains only one pion exchange at order  $p^0$  and the reducible part of the twice iterated one pion exchange, order  $p$ . The former contribution constitutes the LO of the Weinberg's scheme [6, 11]. We are then neglecting important contributions, particularly for the  $P$  and  $D$  waves, from two pion exchange irreducible diagrams, counterterms for the  $P$ -waves at order  $p^2$ , as well as the  $\pi N$  counterterms (which are saturated

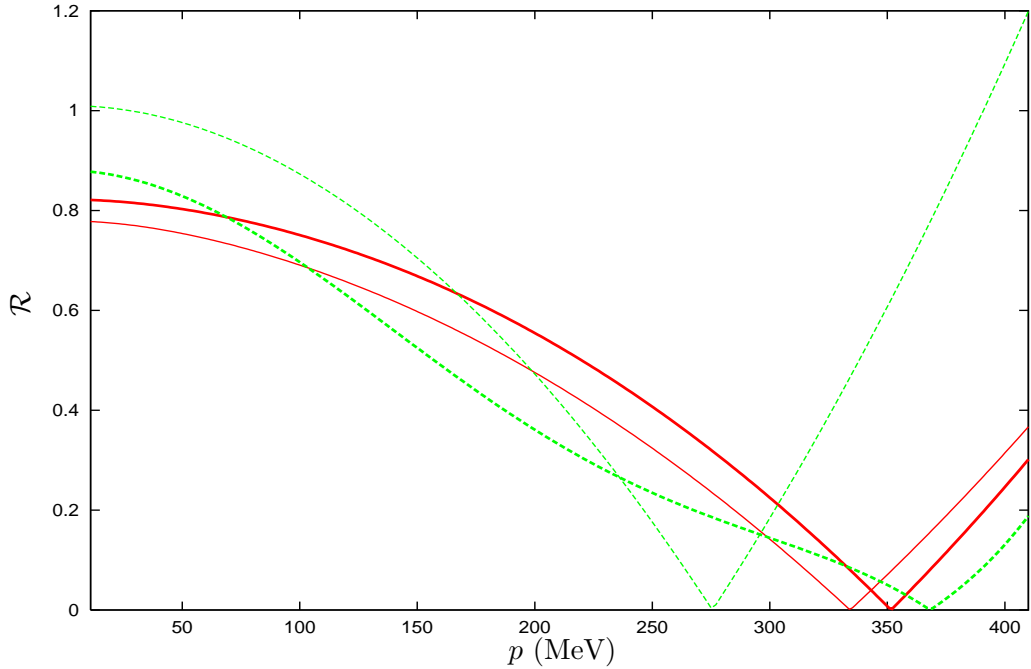


Figure 3:  $|\mathcal{R}^{NLO}|$  (thin solid line),  $|\mathcal{R}^{NNLO}|$  (thick solid line) for the  $S_0^1$  channel and  $|R_{11}^{NLO}/4|$  (thin dashed line) and  $|R_{11}^{NNLO}/4|$  (thick dashed line) for the  $S_1^3$  channel.

to a large extend by the  $\Delta$  isobar), that would appear at order  $p^3$  [11, 21]. Hence a full NNNLO calculation in the KSW scheme should be pursued and then used within our scheme to offer a more complete study of these higher partial waves. For the  $F$  and  $G$  waves and mixing parameters  $\epsilon_2$  and  $\epsilon_3$ , these extra contributions are not so important, see e.g.[21]. This is apparent from our results presented in figs.4 and 5 as well. At the order we are working in these partial waves there are no counterterms and the only free parameters are the subtraction constants  $\nu$ 's, one for each partial wave. In most of the channels, they take arbitrarily large or negative values, that is, any value with modulus typically above the expansion scale  $\Lambda_{xpT} \simeq 0.7 - 1$  GeV gives essentially the same results. Our curves are indeed quite similar to what is obtained in the Weinberg's approach at LO, see [11]. Our results at NNLO, solid lines, improve those of the NLO, dashed lines, except for the  $D_1^3$  where, though the NNLO is better at low  $T_{lab}$ , they depart from data more than the NLO ones for higher energies. They also improve the results from the pure KSW amplitudes, dotted lines, although in these cases, as expected, the resummation effects are not so spectacular as in the S-waves.

## 4 Conclusions

We have established a new analytic expansion in order to treat systematically nucleon-nucleon interactions. The original KSW amplitudes at NLO [18] and NNLO[19] have been used to fix an interacting on-shell kernel,  $\mathcal{R}$ , once the unitarity or right hand cut is resummed to all orders. This kernel is fixed by performing a KSW expansion and then matching with the inverses of the pure KSW amplitudes to any arbitrary given order. As a result, a scheme emerges that treats pions non-perturbatively but in harmony with the KSW power counting, and that dramatically increases both the range of convergence of the original KSW effective field theory and its phenomenological success.

Further applications of the present scheme should be pursued and a KSW N<sup>3</sup>LO calculation should also be performed and then used in our scheme, particularly for a more complete study of the  $P$  and  $D$  partial waves.

### Acknowledgments

I would like to thank E. Epelbaum for interesting discussions that we held in Jülich. I am also grateful to the Benasque Center for Science, where part of this work was done, for its support and enjoyable atmosphere.

## References

- [1] S. Weinberg, *Physica* **A96**, 327 (1979).
- [2] J. Gasser and H. Leutwyler, *Ann. Phys. (N.Y.)* **158**, 142 (1984).
- [3] U.-G. Meißner, *Rep. Prog. Phys.* **56**, 903 (1993);  
G. Ecker, *Prog. Part. Nucl. Phys.* **35**, 1 (1995);  
A. Pich, *Rep. Prog. Phys.* **58**, 563 (1995);  
H. Leutwyler, *Encyclopedia of Analytic QCD*, edited by M. Shifman, World Scientific; hep-ph/0008124
- [4] U.-G. Meißner, *Encyclopedia of Analytic QCD*, edited by M. Shifman, World Scientific; hep-ph/0007092.
- [5] S. Weinberg, *Phys. Lett.* **B251**, 288 (1990); *Nucl. Phys.* **B363**, 3 (1991).
- [6] C. Ordóñez, U. van Kolck, *Phys. Lett.* **B291**, 459 (1992);  
C. Ordóñez, L. Ray and U. van Kolck, *Phys. Rev. Lett.* **72**, 1982 (1994); *Phys. Rev.* **C53**, 2086 (1996);  
U. van Kolck, *Phys. Rev.* **C49**, 2932 (1994).
- [7] T.S. Park, D.P. Min and M. Rho, *Phys. Rev. Lett.* **74**, 4153 (1995); *Nucl. Phys.* **A596**, 515 (1996).
- [8] D.B. Kaplan, M.J. Savage and M.B. Wise, *Nucl. Phys.* **B478**, 629 (1996).
- [9] D. Eiras and J. Soto, nucl-th/0107009.
- [10] S.R. Beane, P.F. Bedaque, W.C. Haxton, D.R. Phillips and M.J. Savage, *Encyclopedia of Analytic QCD*, edited by M. Shifman, World Scientific; hep-ph/0008064.
- [11] E. Epelbaum, W. Glöckle, U.-G. Meißner, *Nucl. Phys.* **A637**, 107 (1998); *Nucl. Phys.* **A671**, 295 (2000).
- [12] G.F. Chew and S. Mandelstam, *Phys. Rev.* **119**, 467 (1960).
- [13] J.A. Oller and E. Oset, *Phys. Rev.* **D60**, 074023 (1999);  
J.A. Oller, *Phys. Lett.* **B477**, 187 (2000);  
J.A. Oller, A. Pich and M. Jamin, *Nucl. Phys.* **B587**, 331 (2000); *Nucl. Phys.* **B622**, 279 (2002); *Eur. Phys. J.* **C24**, 237 (2002).
- [14] J.A. Oller and E. Oset, *Nucl. Phys.* **A620**, 438 (1997), (E)-ibid **A652**, 407 (1999).  
For a general introduction and discussion see J.A. Oller, Invited talk at YITP Workshop on Possible Existence on the sigma meson and its Implications to Hadron Physics, hep-ph/0007349.
- [15] U.-G. Meißner and J.A. Oller, *Nucl. Phys.* **A673**, 311 (2000).

- [16] J.A. Oller, U.-G. Meißner, Phys. Lett. **B500**, 263 (2001); Phys. Rev. **D64**, 014006 (2001).
- [17] A. Dobado, M.J. Herrero and T.N. Truong, Phys. Lett. **B235**, 134 (1990).  
 A. Dobado and J.R. Peláez, Phys. Rev. **D56**, 3057 (1997).  
 T. Hannah, Phys. Rev. **D55**, 5613 (1997).  
 J.A. Oller, E. Oset and J.R. Peláez, Phys. Rev. Lett. **80**, 3452 (1998); Phys. Rev. **D59**, 074001 (1999), (E)-ibid **D60**, 099906 (1999).  
 F. Guerrero and J.A. Oller, Nucl. Phys. **B537**, 459 (1999).  
 A. Gómez Nicola, J. Nieves, J.[arXiv:hep-ph/9805334]. R. Peláez and E. Ruiz Arriola, Phys. Lett. **B486**, 77 (2000).  
 A. Gómez Nicola and J.R. Peláez, Phys. Rev. **D65**, 054009 (2002).
- [18] D.B. Kaplan, M.J. Savage and M.B. Wise, Phys. Lett. **B424**, 390 (1998); Nucl. Phys. **B534**, 329 (1998).
- [19] S. Fleming, T. Mehen and I. Stewart, Nucl. Phys. **A677**, 313 (2000); Phys. Rev. **C61**, 044005 (2000).
- [20] V.G.J. Stoks, R.A.M. Klomp, C.P.F. Terheggen and J.J. de Swart, Phys. Rev. **C49**, 2950 (1994).
- [21] N. Kaiser, R. Brockmann and W. Weise, Nucl. Phys. **A625**, 758 (1997);  
 N. Kaiser Phys. Rev. **C65**, 017001 (2002).
- [22] J.A. Oller, Phys. Rev. **C65**, 025204 (2002).
- [23] U.-G. Meißner, J.A. Oller and A. Wirzba, Ann. Phys. **297**, 27 (2002).

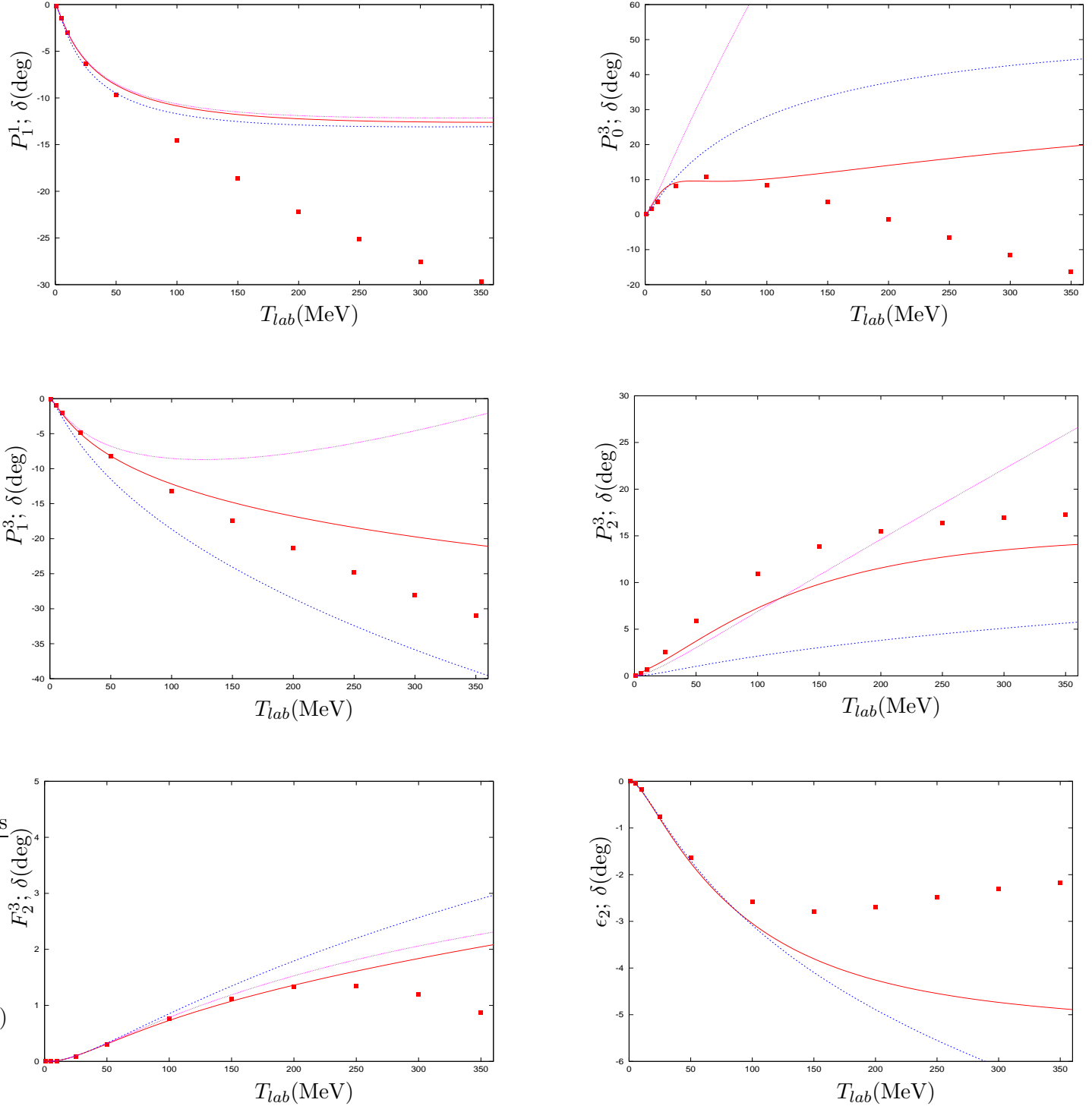


Figure 4: Phase shifts for the  $P_1^1$ ,  $P_0^3$ ,  $P_1^3$ ,  $P_2^3$ ,  $F_2^3$  and  $\epsilon_2$  from left to right and top to bottom, respectively. The dotted line, when present, is the NNLO KSW result [19]. The dashed line represents the NLO results from eq.(2.5). The solid lines are the NNLO results. The data correspond to the Nijmegen partial wave analysis, ref.[20].

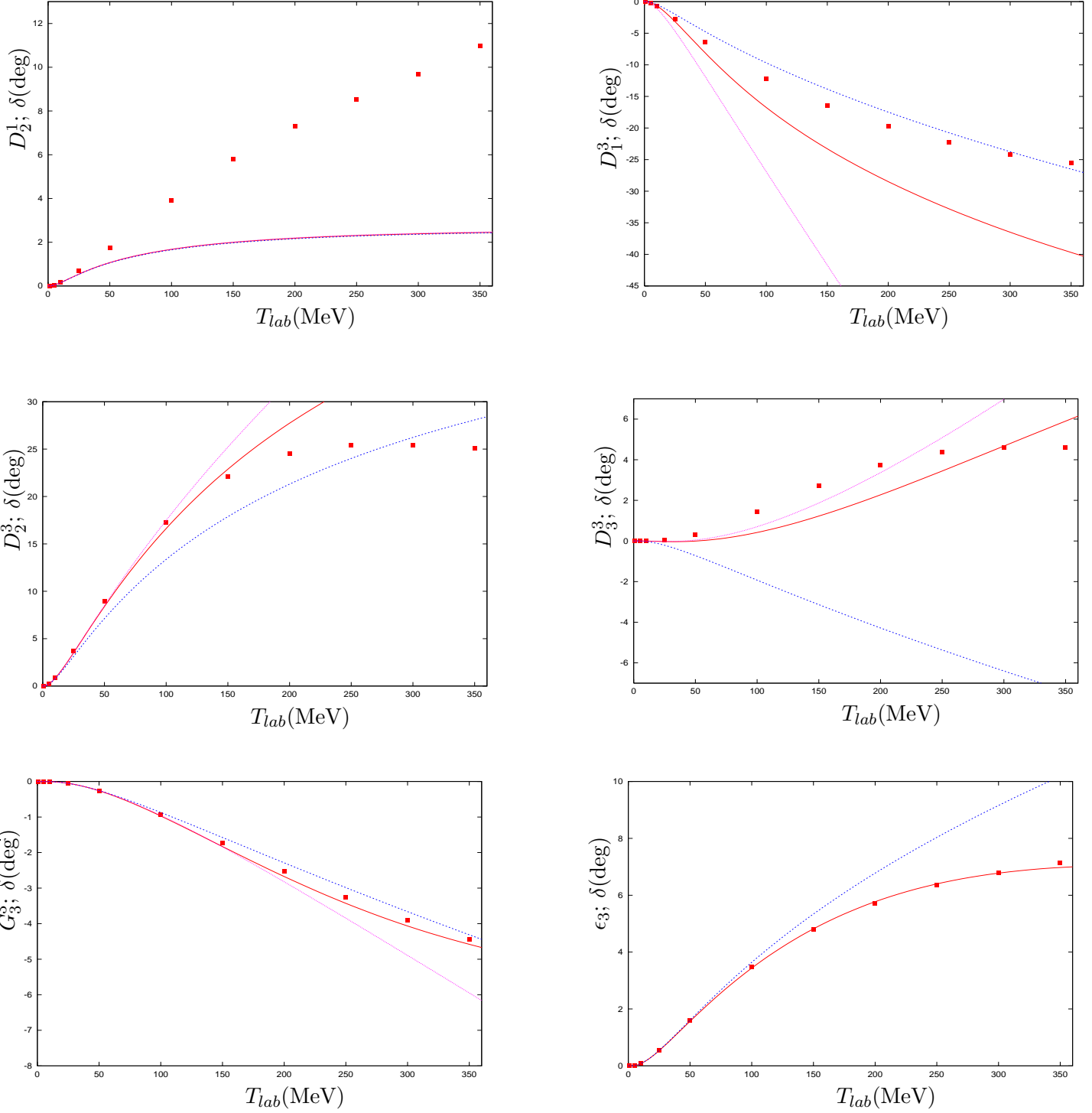


Figure 5: Phase shifts for the  $D_2^1$ ,  $D_1^3$ ,  $D_2^3$ ,  $D_3^3$ ,  $G_3^3$  and  $\epsilon_3$  from left to right and top to bottom, respectively. The dotted line, when present, is the NNLO KSW result [19]. The dashed line represents the NLO results from eq.(2.5). The solid lines are the NNLO results. The data correspond to the Nijmegen partial wave analysis, ref.[20].